

GAS Journal of Engineering and Technology (GASJET)

Volume 2 | Issue 10, 2025

Homepage: https://gaspublishers.com/gasjet-home/



ISSN: 3048-5800

Comparison of Theoretical Analysis and Simulation Results: Determination of Structural Parameters and Displacement Characteristics of Diaphragms in Capacitance Diaphragm Vacuum System

ChangGi Kang, KumHyang Ho, NamChol Yu

Faculty of Electronics, Kim Chaek University of Technology, Pyongyang, Democratic People's Republic of Korea

Received: 30.08.2025 | Accepted: 02.10.2025 | Published: 23.10.2025

*Corresponding Author: NamChol Yu

DOI: 10.5281/zenodo.17422122

Abstract Original Research Article

In this study, computational fluid dynamic method is used to predict and evaluate the flow field and collection performance inside square cyclone separators. Two cyclones with different dust outlet were studied using the Reynolds stress model (RSM). The cyclone flow field pattern has been simulated and analyzed with the aid of static pressure, and velocity components. In addition the cyclone collection efficiency based on one-way discrete phase modeling has been investigated. The obtained results demonstrate that collection performance of the square cyclone separator with vertical dust-outlet is very well. The simulation results agree well with the published experimental results.

Keywords: vacuum gauge, capacitance, diaphragm, vacuum measurement.

Copyright © 2025 The Author(s). This is an open-access article distributed under the terms of the Creative Commons Attribution-NonCommercial 4.0 International License (CC BY-NC 4.0).

1. Introduction

The electrostatic capacitance diaphragm vacuum gage has been widely used in the vacuum apparatus which embrace the oxidizing gas or aggressive gas due to its feature with no relation of the kind of exhausting gases [1]. In addition, the diaphragmatic vacuum gauge is a broadband vacuum guage capable of measuring the pressure of a wide interval from atmospheric pressure to high vacuum depending on the degree of elasticity of the diaphragmatic material, a number of studies have been mainly undertaken to improve the mechanical properties of the diaphragmatic material [2]. Sensor diaphragm material is a thin plate type material with the greater elasticity factor and high mechanical strength; the typical diaphragmatic material is an inconel, which is good for tolerance, thermal and internal oxidative properties, and has less character change at low temperatures [3]. As such, previous studies have mostly suggested an inconel with the best properties as a diaphragmatic material, focused on the direction of the study to measure global band from the low vacuum to high vacuum, and attempted to use other materials excepted it, but other materials have not been introduced significantly because of the degradation of mechanical performance, including elastic coefficients, which is mainly concerned due to the unreasonable broadband vacuum measurement and the non-uniform measurement error[4].

Xiaodong Han et al., evaluated the sensitivity of the vacuum gauge to the measurement range through the operation principle, structure, fabrication and testing of a miniaturized capacitance diaphragm vacuum system [12, 13].

A study has also been published that experimentally evaluated the gas-dependent effect of heat release in



a capacitance diaphragm vacuum system [14].

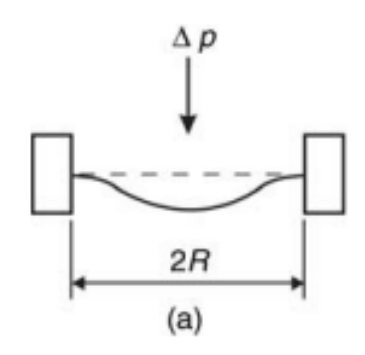
Thus, although the results of studies concerning the structural design and fabrication of vacuum sensors have been reported, there are no theoretical examples of reasonable structural parameters.

On the basis of a comprehensive research analysis of the preceding vacuum measurement methods and vacuum sensors, we have solved theoretical and practical problems arising in designing and fabricating an electrostatic capacitance diaphragm vacuum sensor, a species of capacitance sensors that can be used for long periods even in gases with strong oxidant properties including moisture.

2. Theory

An electrostatic capacitance diaphragm

vacuum gauge is a vacuum gauge that measures vacuum degree by electrically sensing the electrical capacity changes with a fixed electrode placed near the metal diaphragm when the metal diaphragm is displaced by differential pressure acting on either side of the conductive metal diaphragm. In this vacuum gauge, when electronically sensing the deformation of the diaphragm, better sensitivity and accuracy can be obtained than when mechanically sensed. The deformation of the thin-plated circular diaphragm caused by the pressure difference depends on how to support the edge and pull or not it in advance [2,3]. Fig. 1 shows the displacement pattern of the diaphragm by the pressure difference △p which acts perpendicular to the circular diaphragm with radius R.



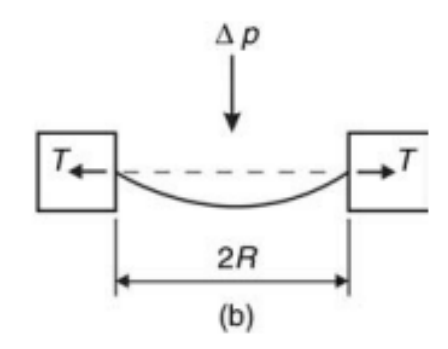


Fig.1. Displacement of the diaphragm by pressure difference

In Fig. a, the edge is tightly fixed by the force perpendicular to the plane, and when $\Delta p=0$, the diaphragm does not act any stress and therefore there is no deformation. In Fig. b, however, a tensile force

T is applied per edge unit length facing outward on a fixed edge, and the diaphragm will be received a radial stress. Fig. 2 shows the principle diagram of the electrostatic capacitance diaphragm vacuum sensor.

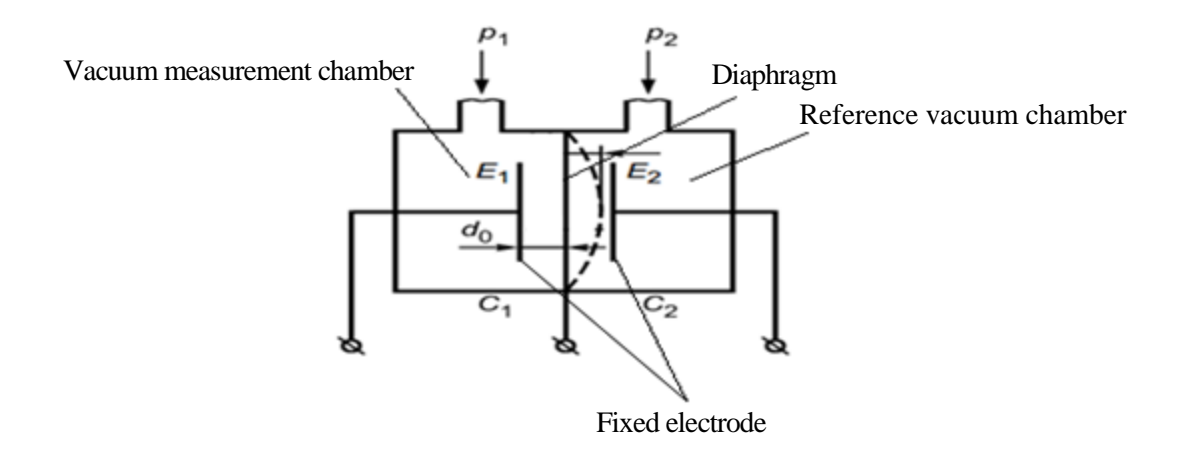


Fig. 2. Schematic of capacitance diaphragm vacuum gauge

As shown in the figure, the body is divided into two parts by a metal diaphragm, where the left region of the diaphragm is connected to bell jar of the exhaustion as a vacuum chamber, and the right region is chosen to be one place lower than the measurement limit vacuum degree as a reference vacuum chamber [4].

In vacuum measurement chamber and the reference vacuum chamber, two electrode E1 and E2 are placed, and they are as far away as the constant distance from the metal diaphragm. Thus, metal diaphragm and electrodes E1 and E2 form capacitors C1 and C2, respectively.

The capacitor produced by the sensor can be approximated by a parallel plate capacitor, so the capacitance of the capacitor formed between the diaphragm and the electrode can be calculated in the following equation [5-8].

$$C = \varepsilon_0 \varepsilon S/d_0$$
 (1)

Here ε_0 and ε are the dielectric constant of vacuum and gas, respectively, and S and d_0 are the fundamental structural parameters of the sensor as the surface area of the capacitor electrode, and the effective interval between the diaphragm and the electrode. The electrode surface area is chosen at a size of about 1 cm² so that the flexible diaphragm can be displaced sufficiently when the interval between the diaphragm and the electrode is hundreds of μ m.

When a pressure difference is applied to the sensor diaphragm, the diaphragm is displaced toward a low pressure vacuum measurement chamber, where the interval between the diaphragm and the electrode changes, and the capacitance value of the capacitance is changed and therefore the vacuum can be measured. When the vacuum of a reference vacuum chamber is provided with a high vacuum of approxiately 0, the measured vacuum degree is an absolute pressure, so this sensor becomes an absolute vacuum sensor. On the other hand, if the initial vacuum of the reference vacuum chamber is provided with some constant vacuum, the measured vacuum is the difference between the measurement chamber and the pressure of the reference vacuum chamber, so this sensor becomes a differential vacuum sensor.

According to elastic theory, the maximum displacement of the diaphragm occurs at the center of the diaphragm, and this value is proportional to the pressure difference acting on the diaphragm. An electrostatic capacitance diaphragm vacuum gauge is a vacuum gauge that is very suitable for vacuum measurement of vacuum distillation or vacuum drying devices that are difficult to use a pyrani vacuum gauge or thermo-charged vacuum gauge. During vacuum drying, gases with strong oxidative properties, including vapor or moisture, are exhausted. Therefore, a number of technical problems arise in the measurement of vacuum-

drying devices, which can be measured accurately, regardless of the type of gas, using an electrostatic capacitance diaphragm vacuum gauge. In the case that the diaphragm is exerted by a pull force F per

edge unit length facing outward to the fixed edgeand force is acted with radius, and the displacement x decreases with radius r, and in the center (r=R), the displacement x0 is the follow[10].

$$x_0 = \frac{R^2}{4F} \Delta p \tag{2}$$

In addition, the natural vibration frequency of a pulled diaphragm made of material with a density ρ is as follows.

$$f = \frac{0.7655}{2R} \sqrt{\frac{F}{\rho h}} \tag{3}$$

In the expression, *h* is the thickness of the diaphragm.

The initial interval X between the diaphragm and the electrode should be slightly larger than the maximum displacement x_0 of the diaphragm. It is because a pressure greater than the maximum marginal pressure difference that can act on the diaphragm may act, causing the diaphragm to be shunted with the electrode, resulting in the destruction of the sensor. The displacement for excess pressure prevention is reduced to 25%, determining the interval X between the diaphragm and the electrode.

3. Analysis of the displacement properties of the diaphragm and determining of structure properties

3.1 Bending properties of a thin sheet with a constant thickness under symmetry force

In the designed electrostatic capacitance diaphragm vacuum gauge, the edge of the circular diaphragm is in a state supported by a certain force and the equally distributed force along the concentric circle of the circular diaphragm acts perpendicular to the diaphragm [11].

Fig. 3 shows an equally distributed force acting on thin diaphragm.

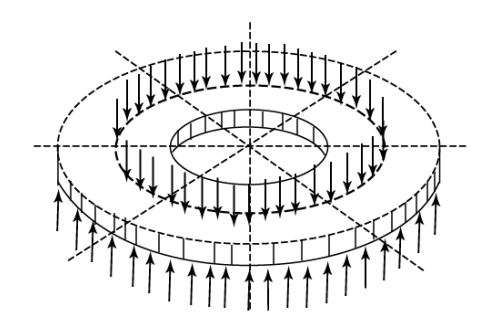


Fig.3. Uniformly distributed force along a concentric circle acting on a thin diaphragm

The deformation and stress state of the diaphragm is symmetrical for the central axis Z of the diaphragm, and the middle surface is a elastic surface of the diaphragm, forming some rotational surface. Fig. 4 shows the deformation and stress state of the diaphragm by force acting on the thin diaphragm.

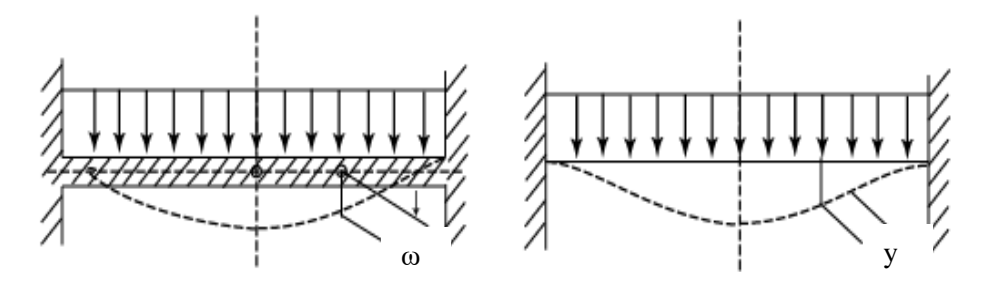


Fig.4. Strain and stress state when the force was acted the diaphragm

To interpret the displacement properties of the diaphragm, the following assumption was proposed.

Assumption 1.

When the Z-direction displacement ω of any point above the middle surface is much smaller compared to the thickness h of the plate, the middle surface of the plate is only bending, does not pull, and the radial displacement of the points on the middle plane neglects.

Assumption 2

Before deformation, the points on any

straight line perpendicular to the middle surface of the plate are placed on a straight line perpendicular to the middle plane (elastic surface) after deformation.

Assumption 3.

The normal stress in the plane parallel to the middle plane is neglected relative to the stress of the plane perpendicular to the middle plane, and no interaction exists between the layers of the plate.

Based on this assumption, we considered the element ABST of the diaphragm with radial dimensions dr.

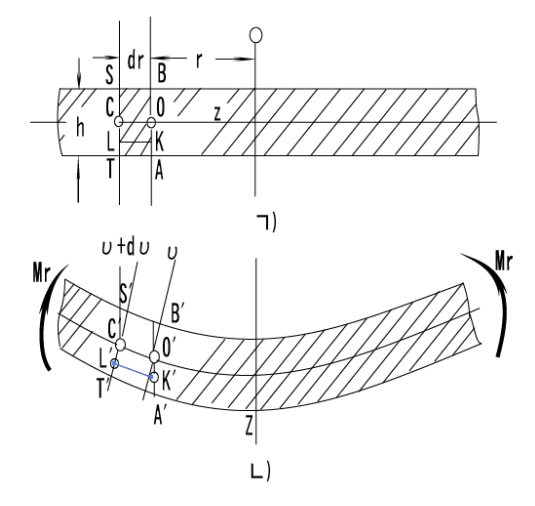


Fig.5. Element of the diaphragm



By Assumption 1, after deformation points O and C also will be at the distance of r, r+dr from the Z-axis, as before deformation, and the normal AOB parallel to the Z-axis before deformation by Assumption 2 rotates as much as the angle v by deformation of the element, while a straight line perpendicular to the

middle surface.

The radial line KL at a distance of z from the middle surface of the diaphragm displaces to the position of K'L' after deformation, and its relative stretching is as follows [7].

$$\varepsilon_r = \frac{K'L' - KL}{KL} = \frac{LL' - KK'}{KL} = \frac{z(v + dv) - zv}{dr} = \frac{zdv}{dr}$$
(4)

The circumferential length change et of the K point can be easily calculated by comparing the length of the circumference with the K point after deformation and deformation.

$$\varepsilon_t = \frac{2\pi(r+zv) - 2\pi r}{2\pi r} = z\frac{v}{r} \tag{5}$$

From Hooke's law the relationship between stress and strain is;

$$\varepsilon_r = \frac{1}{E}(\sigma_r - \nu \sigma_t)$$
$$\varepsilon_t = \frac{1}{E}(\sigma_t - \nu \sigma_r)$$

Where E is the elasticity coefficient and v is the transverse deformation coefficient.

When the stress is expressed as a strain in the upper expression, it is the follow:

$$\sigma_r = \frac{E}{1 - v^2} (\varepsilon_r + v\varepsilon_t)$$
$$\sigma_t = \frac{E}{1 - v^2} (\varepsilon_t + v\varepsilon_r)$$

Substituting Equation (4), (5) to this expression;

$$\sigma_{r} = \frac{Ez}{1-\nu^{2}} \left(\frac{dv}{dr} + \nu \frac{v}{r} \right)$$

$$\sigma_{t} = \frac{Ez}{1-\nu^{2}} \left(\frac{v}{r} + \nu \frac{dv}{dr} \right)$$
(6)

From Eq. (6), it can be seen that the normal stress of the middle plane (z=0) is zero, the distribution of the stress is proportional to the distance from the middle surface, the tensile stress on one side of the middle and the compressive stress on the other.

Prior to considering the balance of the element $ABSTA_1B_1S_1T_1$ of the disc, we considered the speed force acting on the surfaces of the element. When the shearing force in the Z direction by tangential stress on the surface ABB1A1 acts, it is called the density of the cut force that is the magnitude of the force

acting on unit length of the arc $rd\varphi$ and denotes as Q[kg/cm]. Thus, the cut force acting on the surface ABB₁A₁ is $Qrd\varphi$ and the cut force acting on the surface STT₁S₁ is $Qrd\varphi+d(Qrd\varphi)$. If the cut force acting on the cylindrical surface of a ring element of radius r directed to the positive direction of the Z axis, then the direction of this force is fixed the direction (+).and the action and reaction are always the opposite direction, so the cutforce of positive on the outer cylinder side of the ring element is oriented opposite to the Z axis.

The normal stresses acting on each side of the element can be reduced to the joint force and bending moment in the normal direction. The sum force of the

normal direction acting on ABST (or $A_1B_1S_1T_1$) and the sum force of normal stresses acting on the principal surface becomes zero.

$$N_{ABST} = \int_{-\frac{h}{2}}^{\frac{h}{2}} \sigma_t dr dt = \frac{Edr}{1 - v^2} (\frac{v}{r} + v \frac{dv}{dr}) \int_{-\frac{h}{2}}^{\frac{h}{2}} z dz = 0$$

$$N_{ABB_1A_1} = \int_{-\frac{h}{2}}^{\frac{h}{2}} \sigma_r r d\varphi dz = \frac{Erd\varphi}{1 - v^2} \left(\frac{dv}{dr} + v\frac{v}{r}\right) \int_{-\frac{h}{2}}^{\frac{h}{2}} z dz = 0$$

The magnitude of the moment per unit length of the radial and circumferential direction is called the bending moment and denotes by M_r , M_t , respectively. The bending moment at the surface ABST and $A_1B_1S_1T_1$ is M_tdr , $M_rrd\varphi$ and the bending moment at the surface ABB₁A₁ is $M_rrd\varphi+d(M_rrd\varphi)$ and the relationship between the bending moment and the stress is as follows.

$$M_r r d\varphi = \int_{-\frac{h}{2}}^{\frac{h}{2}} \sigma_r r d\varphi z dz, M_t dr = \int_{-\frac{h}{2}}^{\frac{h}{2}} \sigma_t dr z dz$$
 (6)

Hence, introducing $M_r = \int_{-\frac{h}{2}}^{\frac{h}{2}} \sigma_r z dz$, $M_t = \int_{-\frac{h}{2}}^{\frac{h}{2}} \sigma_t z dz$ to eq(5), the result is that

$$M_r = \frac{E}{1-v^2} \left(\frac{dv}{dr} + v \frac{v}{r} \right) \int_{-\frac{h}{2}}^{\frac{h}{2}} z^2 dz = \frac{Eh^3}{12(1-v^2)} \left(\frac{dv}{dr} + v \frac{v}{r} \right), M_t = \frac{Eh^3}{12(1-v^2)} \left(\frac{v}{r} + v \frac{dv}{dr} \right)$$

If $\frac{Eh^3}{12(1-v^2)} = D$ is the cyclinder rigidity, bend moment is the same as the following.

$$M_r = D(\frac{dv}{dr} + v\frac{v}{r}), M_t = D(\frac{v}{r} + v\frac{dv}{dr})$$
 (7)

At the point where the Z coordinates are positive (+), when the bending moment which the stress acts as a tensile stress by a positive orientation is selected, from Equation (7), t relationship holds between the bending moment, M_r , M_t and the rotation angle v is the follow.

$$v = \frac{(M_t - \nu M_r)r}{D(1 - \nu^2)dr} = \frac{12r}{Eh^3} (M_t - \nu M_r)$$
 (8)

When the forces acting on the element to the Z-axis is mapped.

$$Qrd\varphi - [Qrd\varphi + d(Qrd\varphi)] + Pr d\varphi dr = 0$$

So ordering the expression;

$$\frac{d(Qr)}{dr} = Pr \tag{9}$$

Sum of the moments that all the forces acting on the element $ABSTA_1B_1S_1T_1$ give to the Y axis tangent to the arc of the radius r of the middle surface is the follow:

$$M_r r d\varphi - [M_r r d\varphi + d(M_r r d\varphi)] + Pr d\varphi dr \frac{dr}{2} + 2M_t dr sin \frac{d\varphi}{2} - [Qr d\varphi + d(Qr d\varphi)]dr = 0$$

The following are the results of ordering the expression and neglecting the microvolume of the high order.



$$M_t - \frac{d[M_r r]}{dr} = Qr \tag{10}$$

The sum of the mapping component to the Z-axis of all forces acting on the elements of the diaphragm is $2\pi rQ - \int_0^{2\pi} \int_0^r p \, r \, d\varphi dr + P = 0$, thus $Q = \frac{\pi r^2 p - P}{2\pi r} (kg/cm)$ and if substrating Eq(7) to Eq(10), the result is that

$$\frac{d^2v}{dr^2} + \frac{1}{r}\frac{dv}{dr} - \frac{v}{r^2} = -\frac{Q}{D} \text{ or } \frac{d}{dr} \left[\frac{1}{r}\frac{d(vr)}{dr} \right] = -\frac{Q}{D}$$
 (11)

integrating

$$v = C_1 r + \frac{C_2}{r} - \frac{1}{Dr} \int [r \int Q dr] dr$$
 (12)

Here C1, C2 are integral constants determined by boundary conditions. If the rigidity of the panel is strong, relationship between displacement ω and angle of rotation is that $\frac{d\omega}{dr} = \tan(\pi - \upsilon) \approx -\upsilon$. From this equation, the displacement is as the following.

$$\omega = C_3 - \int v dr \tag{13}$$

From Eq(4), (7)

$$\sigma_t = \frac{12M_t z}{h^3}$$

$$\sigma_r = \frac{12M_r z}{h^3}$$
(14)

Here, the strongest direct stress is generated at $z=\pm 0.5h$.

$$\sigma_{r_{\text{max}}} = \frac{6M_r}{h^2}$$

$$\sigma_{t_{\text{max}}} = \frac{6M_t}{h^2}$$

The integral constant in Equation (12), (13) is determined by the boundary condition.

At the fixed support boundary v=0 and from Eq. (7)

$$M_t = vM_r$$
 (15)

At the free or free support boundary.

$$M_r = \pm m$$
 (16)

Here $\pm m$ is the moment of the external force acting on the boundary under consideration or the outer concentration moment.

If there is no moment on this boundary, it is the follow;

$$M_r=0$$
 (17)

3.2 The thickness and displacement calculation of the diaphragm

The diaphragmatic vacuum sensor is a kind of vacuum sensor that performs vacuum measurement using



the displacement properties of the diaphragm by a pressure difference acting on the diaphragm. In this design, electrode type is selected to concentric type and the main structure is showed in Fig.6.

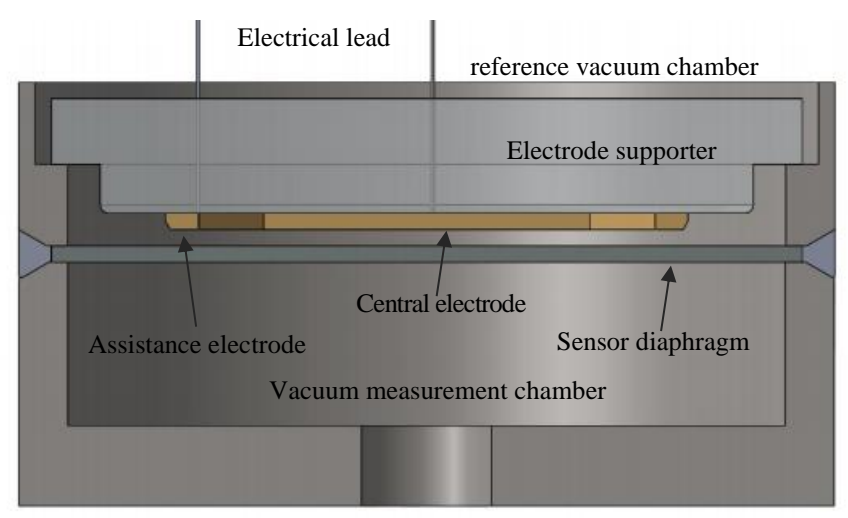


Fig. 6. Structure of the sensor

Electrode

As you can see in the figure, the sensor consists of a reference vacuum chamber consisting of a diaphragm and a sensor body, a vacuum chamber and an electrode structure, and the electrode structure consists of a central electrode and a ring electrode, where the electric capacitance value of the variable capacitor, by causing between the electrodes and the diaphragm, is C1 and C2, respectively. As it was intended to develop a vacuum gauge capable of measuring the vacuum level of the basal vacuum band, the vacuum diagram of the reference vacuum chamber should be provided at 100 Pa [4]. When the pressure difference △p is applied to the diaphragm

shown in the figure, let us ignore the cylinder part of the box and the bending of the flange and determine the thickness h of the diaphragm and the maximum displacement of the diaphragm to satisfy the strength conditions. The tensile tolerance stress is $[\sigma] = 200$ MPa, the ratio of the tensile yield limit and the compressive yield limit is 0.8, the elasticity coefficient of the material is $E=2\times10^5$ Mpa, and the transverse deformation coefficient is $\mu=0.25$.

From the structure of the sensor, the diaphragm can be seen as a disk which the outer boundary is fixed and constant pressure operates.

The shearing force is $Q = \frac{\pi r^2 p}{2\pi r} = \frac{pr}{2}$, $(0 \le r \le R)$, which is assigned to Eq. (11) and $\frac{d}{dr} \left[\frac{1}{r} \frac{d(vr)}{dr} \right] = -\frac{Q}{D} = -\frac{pr}{2D}$. The integration of this equation is $v = C_1 r + \frac{C_2}{r} - \frac{pr^3}{16D}$ and $C_2 = 0$ because there is no hole in the center of the plate.

Considering the fixed support boundary condition v=0 (r=R), since $C_1 = \frac{pr}{16D}(R^2 - r^2)$, the rotation angle is denoted as the following.



$$v = \frac{pr}{16D}(R^2 - r^2)$$

Fig. 7 shows the stress state at the center of the diaphragm and on the surface of the plate.

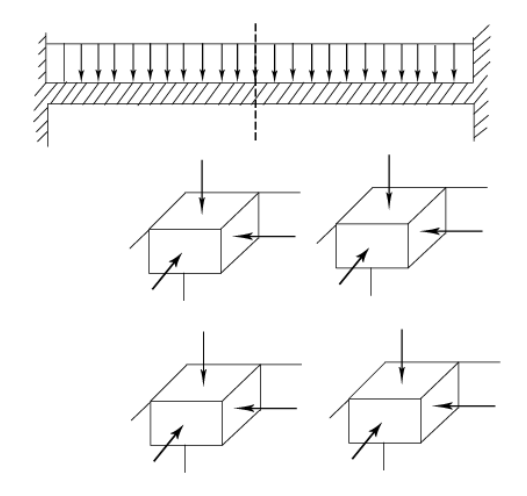


Fig. 7.Stress status at the center and end of the diaphragm

The stress at the central point of the surface is found by Equation (14), at point A, $\sigma_1 = -p$, $\sigma_2 = \sigma_3 = -\frac{3}{8}(1 + \nu)\frac{PR^2}{h^2}$, and $|\sigma_1|$ is much smaller than $|\sigma_3|$, thus $\sigma_1 \approx 0$. In the same way, the stress at different points is calculated, at point B, $\sigma_1 = \sigma_2 = -\frac{3}{8}(1+\nu)\frac{pR^2}{h^2}$, $\sigma_3 = 0$, at point C, $\sigma_1 = \frac{3}{4}\frac{pR^2}{h^2}$, $\sigma_2 = \frac{3}{4}\nu\frac{pR^2}{h^2}$, $\sigma_3 = 0$, at point D, $\sigma_1 = 0$, $\sigma_2 = -\frac{3}{4}\nu\frac{pR^2}{h^2}$, $\sigma_3 = -\frac{3}{4}\frac{pR^2}{h^2}$.

Hence, the results of calculating the diffraction stress at different points of the diaphragm are as follows:

$$\begin{split} \sigma_{eq(A)} &= -0.8[-\frac{3}{8}(1+\nu)\frac{pR^2}{h^2}] = 0.384\frac{pR^2}{h^2} & \text{Point A} \\ \sigma_{eq(B)} &= \frac{3}{8}(1+\nu)\frac{pR^2}{h^2} = 0.48\frac{pR^2}{h^2} & \text{Point B} \\ & & & & \\ & & & \\ & & & & \\ &$$

According to Mor's theory of strength, a plastic deformation begins when the largest value of the reduced $\sigma_{eq} = \sigma_1 - \overline{\nu}\sigma_3$ stress reaches a certain value.

After all, when the pressure is applied to the sensor, the thickness h is calculated by the strength condition as

the C point with the greatest diffraction stress is the most dangerous point.

$$\frac{3}{4} \frac{pR^2}{h^2} \le [\sigma]$$

$$h^2 \ge \frac{0.75 \cdot p \cdot R^2}{[\sigma]} \tag{19}$$

Substituting (18) to Eq. (13) achieves the following result:

$$\omega = C_3 - \frac{p}{16D} \int r(R^2 - r^2) dr = C_3 - \frac{p}{16D} (\frac{R^2 r^2}{2} - \frac{r^4}{4})$$

Considering $\omega=0$ in the boundary condition r=R, since $C_3 = \frac{pR^2}{64D}$, where $\omega = \frac{p}{64D}(R^2 - r^2)^2$, the maximum displacement of the diaphragm occurs at the center of the plate, so that

$$\omega_{max} = \frac{3}{16} \frac{1 - \nu^2}{E} \frac{pR^4}{h^2}$$
 (20)

The results of calculating the thickness of the diaphragm and the maximum displacement of the diaphragm along the diameter of the different diaphragm by Equations (19) and (20) are shown in Table 1.

Table 1. Maximum displacement value of the diaphragm according to the diameter and thickness of the diaphragm

Diameter of diaphragram(D)	Thickness of diaphragram(h)	Maximum displacement(w)
15	0.14	0.09
20	0.19	0.11
25	0.24	0.13
30	0.29	0.1815
35	0.338	0.34
40	0.3871	0.426
45	0.435	0.461
50	0.048	0.5

In order to accurately measure the capacitance of the capacitance formed between the diaphragm and the electrode, the capacitance value should be as great as possible and the maximum displacement of the diaphragm following the pressure difference on both sides of the diaphragm should be as great as possible.

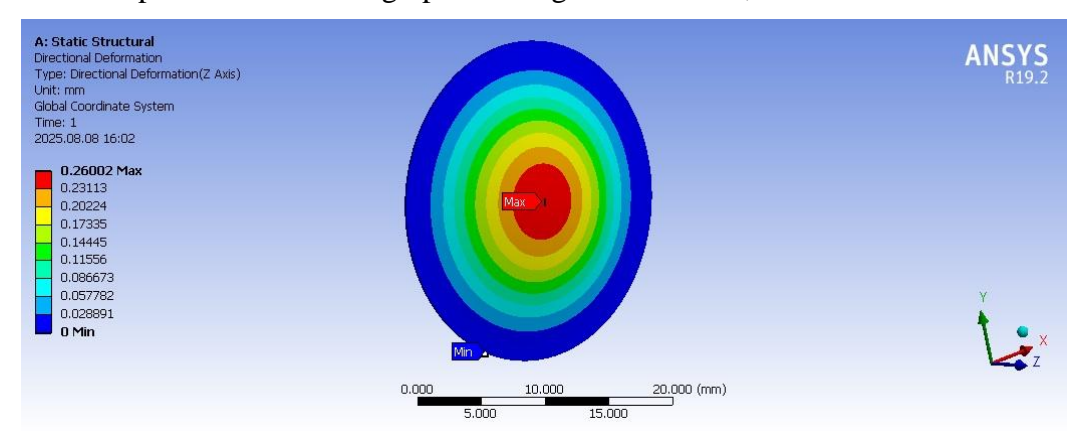
In order to satisfy these conditions, the diameters of the diaphragm must be as large as possible, as shown in Table 1, so that the force of pulling the edge of the diaphragm must be great. Taking into account the tensile force of the structure that fixes the diaphragm at 30 mm, the diaphragm is 0.3 mm thick and the maximum displacement of the diaphragm is 0.18 mm.

4. ANSYS simulation results

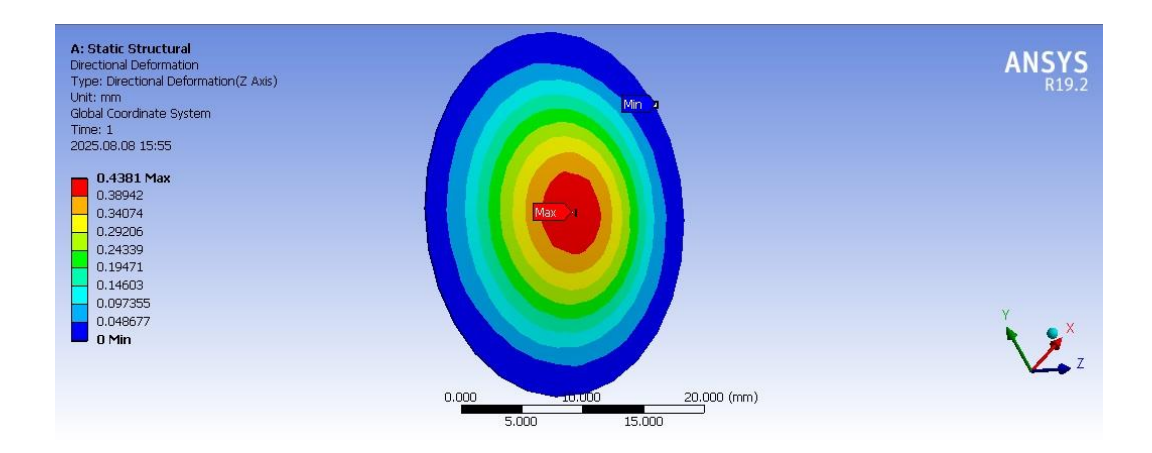
Through simulation analysis by ANSYS, the

results of calculation of maximum displacement versus diameter and thickness of the diaphragm in the capacitance diaphragm vacuum system considered above theoretically are verified.

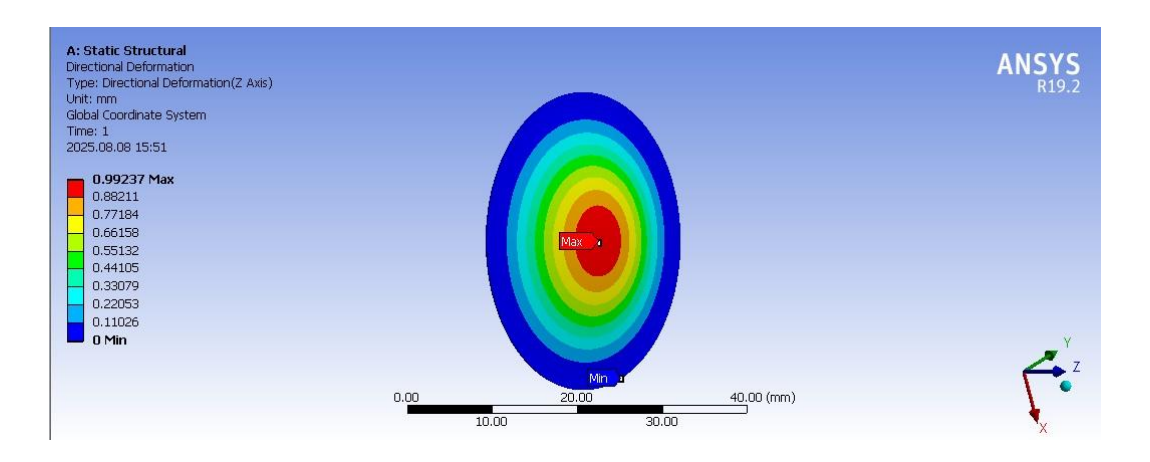
The simulation was performed in a 3D graphics using ANSYS 19.2, and the results are shown in Fig. 8.



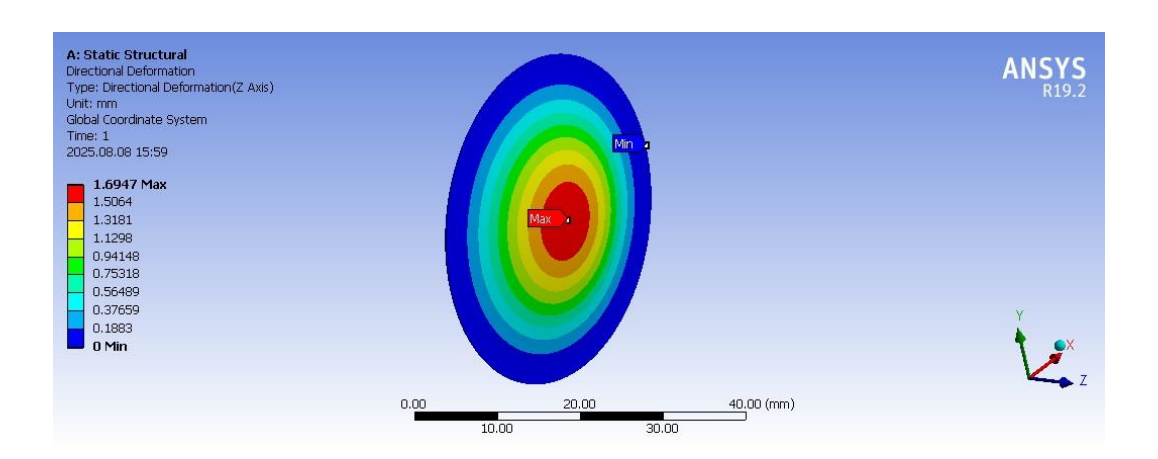
a)



b)



c)



d)

Fig. 8. ANSYS simulation results for maximum displacement of capacitance diaphragm vacuum gauge.

a) diaphragm diameter D-25 mm, thickness h-0.2 mm; b) D-30 mm, h-0.2 mm; c) D-35 mm, h-0.2 mm; d) D-40 mm, h-0.2 mm.

The simulation results are compared with the theoretical analysis results in Table 2.

Table 2 Comparison of theoretical and simulation results

Diameter of diaphragram(D)	Thickness of diaphragram(h)	Maximum displacement(w)	
		Theoretical	Simulation
25	0.2	0.15	0.26
30	0.2	0.26	0.43
35	0.2	0.73	0.99
40	0.2	1.35	1.67

As can be seen in Table 2, the maximum displacement of the membrane increased with the diaphragm diameter when the thickness of the membrane was constant, which was the same trend in both theoretical and simulation analyses.

The numerical difference between the theoretical and simulation analysis is related to the number of mesh elements in the simulation when the finite element analysis is performed.

Although the calculation accuracy can be increased

by increasing the number of mesh elements, the calculation time is increased, and the above results can be used to fully verify the trend of maximum displacement variation, which can ensure the accuracy of the theoretical analysis.

As the theoretical analysis and simulation results show, in order to accurately measure the capacitance of the capacitor formed between the membrane and the electrode, the capacitance value should be as large as possible and the maximum displacement of the membrane with the pressure difference acting on both sides of the membrane should be as large as possible.

To satisfy these conditions, the diameters of the diaphragms should be as large as possible, as shown in Tables 1 and 2, which would result in a large pull-out force at the edges of the diaphragm.

Considering the tension of the structure that holds the diaphragm, the diaphragm diameter is chosen to be 30 mm, with the diaphragm thickness being 0.3 mm and the maximum displacement of the diaphragm being 0.18 mm.

5. Conclusion

In this paper, we analyze the performance of capacitance diaphragm vacuum sensor. the determine the mathematical model to calculate the diaphragm diameter, thickness, and maximum displacement of the diaphragm along measurement range, and determine the structural parameters of the sensor for basic vacuum measurement. To measure the capacitance of the capacitor formed between the diaphragm and the electrode accurately, the capacitance value should be as large as possible and the maximum displacement of the diaphragm with the pressure difference acting on both sides of the diaphragm should be as large as possible.

Considering the tension of the structure that fixes the diaphragm, the diaphragm diameter is chosen to be 30 mm, and the corresponding thickness and maximum displacement of the diaphragm are calculated, with a thickness of 0.3 mm and a maximum displacement of 0.18 mm.

Through theoretical calculations and simulations, the maximum displacement characteristics with diaphragm diameter and thickness were analyzed, and the trend was consistent.

REFERENCES

1. Leatitia Lago, "A rugged, high precision capacitance diaphragm low pressure gauge for cryogenic use", Review of Scientific Instruments 85, 015108 (2014); doi:

- 10.1063/1.4861358
- 2. V. N. Gorobei and E. K. Izrailov, "A STANDARD LOW ABSOLUTE PRESSURE MEMBRANE- CAPACITANCE MANOMETER", Measurement Techniques, Vol. 54, No. 4, July, 2011.
- 3. J.M. Hidalgo, "Uncertainties in calibration using capacitance diaphragm gauges as reference standard", Vacuum 82 (2008) 1503–1506
- 4. Mercede Bergoglio, "Some considerations on handling the calibration results of capacitance membrane gauges", Vacuum 60 (2001) 153-159
- 5. K. Jousten, "On the stability of capacitance-diaphragm gauges with ceramic membranes", J. Vac. Sci. Technol. A 29,,1..., Jan/Feb 2011.
- 6. Barthélémy Daudé, "On the gas dependence of thermal transpiration and a critical appraisal of correction methods for capacitive diaphragm gauges", Vacuum 104 (2014) 77-87.
- 7. Kenichi Iwata, "Modification of Takaishi—Sensui formula for a diaphragm gauge system connected by an arbitrary length pipe", Vacuum, Vol. 84, Issue 11, 2010, pp. 729-733.
- 8. Kenta Arai, "Measurement of volume change induced by a bulging of a diaphragm inside a differential type capacitance diaphragm gauge", Measurement, Vol. 48, 2014, pp. 149-154.
- 9. Shin-Ichi Nishizawa, "DSMC analysis of thermal transpiration of capacitance diaphragm gauge", Vacuum, Vol. 67, 2002, pp. 301-306.
- 10. David S. Betts, "Modern Vacuum Physics", CRC Press, 2010,1-260.
- 11. S.P.Timoshenko, "Theory of elastisity", McGraw-Hill,1970, 30-150
- 12. Xiaodong Han, Gang Li et al., "Miniature capacitance diaphragm for absolute vacuum measurement", Measurement 194 (2022) 110851
- 13. Xiaodong Han, Gang Li et al., "Differential MEMS capacitance diaphragm vacuum gauge with high sensitivity and wide range", Vacuum



191(2021) 110367

Barthelemy Daude, Hadj Elandaloussi et al., "On the gas dependence of thermal transpiration and a critical appraisal of correction methods for capacitive diaphragm gauges", Vacuum 104 (2014) 77-87